Single-crystal aluminum nitride nanomechanical resonators

A. N. Cleland[a)]
Department of Physics and The Institute for Quantum Engineering, Science and Technology, University of California at Santa Barbara, Santa Barbara, California 93106

M. Pophristic and I. Ferguson
Emcore Corporation, 145 Belmont Drive, Somerset, New Jersey 08873

(Received 21 May 2001; accepted for publication 3 July 2001)

Aluminum nitride is a light, stiff, piezoelectrically active material that can be epitaxially grown on single-crystal Si. AlN is beginning to play a role in the integration of semiconducting electronic and surface acoustic wave devices, and may prove useful for the integration of other types of mechanical devices as well. We describe the growth and subsequent electron-beam patterning and etching of epitaxial AlN-on-silicon films into nanomechanical flexural resonators. We have measured resonators with fundamental mechanical resonance frequencies above 80 MHz, and quality factors in excess of 20 000. © *2001 American Institute of Physics.* [DOI: 10.1063/1.1396633]

Aluminum nitride is proving to be a useful material in the semiconductor industry, as it can be grown epitaxially on ⟨111⟩ Si substrates, typically by metalorganic chemical vapor deposition (MOCVD), forming high quality, smooth films with the c axis oriented along the growth direction. AlN is a very light ($\rho = 3255\,\mathrm{kg/m^3}$), stiff material, with a Young's modulus of 345 GPa and a c-axis sound velocity of 11.4 km/s. The large piezoelectric constant $e_{33} = 1.5\,\mathrm{C/m^2}$ corresponds to an electromechanical coupling constant $k^2 = 6.5\%$.[1] Aluminum nitride is fracture resistant and chemically nonreactive, with negligible etching rates when exposed to most strong acids and bases.[2]

This material is a clear candidate for the integration of surface-acoustic wave devices on chip with silicon-based electronics. In addition, it can be used to fabricate submicron-scale cantilevers and flexural beams. Such suspended, mechanically active structures allow applications in force microscopy, optical couplers, and stable oscillators and filters. Other materials under development for these applications include Si, both single crystal and polycrystalline, polycrystalline silicon nitride, GaAs, and silicon carbide.[3–10] Mechanical actuation and sensing in most of these materials relies on electrostatic, optical, or magnetomotive techniques, which suffer from poor coupling and implementation difficulties. Aluminum nitride, by contrast, provides both the possibility for very high resonance frequencies and piezoelectric actuation.

We have developed a method to fabricate radio frequency flexural resonators from single-crystal AlN films. Here we describe the fabrication process, as well as measurements demonstrating fundamental resonance frequencies above 80 MHz and very high quality factors, in excess of 2×10^4.

The AlN films samples were grown on ⟨111⟩ Si wafers in a multiwafer, rotating disk MOCVD system under low-pressure conditions. Triethylaluminum (TEA) and ammonia (NH_3) were used as the Al and N precursors, with H_2 as the carrier gas. Low pressures were used to accommodate the low vapor pressure of TEA, and to minimize pre-reactions. Prior to buffer layer growth, the Si wafers were etched for 20 s in 10% hydrofluoric acid. The wafers were then heated for 10 min at 900 °C in a H_2 atmosphere, leaving an atomically clean surface for epitaxy. An AlN nucleation layer (25 nm thick) was then grown at an approximate surface temperature of 550 °C and TEA and NH_3 flows of 0.6 μmoles/min and 1.1 moles/min, respectively. The AlN epilayer was then grown at 1100 °C, with a TEA flow of 0.9 μmoles/min, establishing a V/III ratio of 12 000; a growth rate of 0.15 μm/h can thereby be achieved. Film thicknesses were measured by optical interferometry to be $t = 0.17\,\mu$m. A more detailed description of the growth system and process can be found elsewhere.[11]

Flexural resonators were fabricated using a combination of optical and electron beam lithographies. Optical lithography was used to define a liftoff pattern for large-scale wire-bond pads, which consisted of a 3 nm thick Ti adhesion layer followed by a 110 nm thick Au film. Electron-beam lithography was then used to define a liftoff pattern for a metal electrode that runs along the length of each resonator for magnetomotive excitation.[5] The electrode comprised a 3 nm Ti adhesion layer, a 35 nm Au film, and a 60 nm Ni film; the Ni served as an etch mask for the anisotropic reactive ion etch of the AlN. Beam lengths ranged from 3.6 to 5.9 μm, with 0.2 μm widths. The ends of the beams were defined by a step increase in the width to 2.4 μm.

The electrode pattern was transferred to the AlN film using anisotropic Cl_2-based reactive ion etching (RIE). Samples were placed in a parallel-plate load-locked RIE chamber, which was pumped to 5×10^{-7} Torr. Chlorine gas was admitted at 10 sccm, with a chamber pressure of 5 mTorr. A rf plasma was ignited with 200 W of rf power, yielding a substrate voltage of 400 V. The AlN etch rate was approximately 150 nm/min, with very vertical sidewalls. The etch rate for the Si substrate and the Ni mask was negligible in these conditions.

The Ni was then removed using a commercial Ni etchant,[12] and the structures released by etching the Si sub-

a)Author to whom correspondence should be addressed; electronic mail: cleland@physics.ucsb.edu

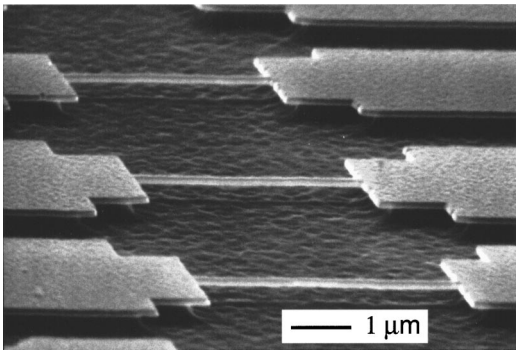

FIG. 1. Series of four AlN beams, with the undercut lengths ranging from 3.9 to 5.6 μm. The beams are 0.17 μm thick, and the widths are 0.2 μm, increasing to widths of 2.4 μm at either end.

strate with an isotropic wet etchant [5 parts ammonium fluoride:120 parts nitric acid:60 parts de-ionized (DI) water[13]]. A 15 s etch was sufficient to mechanically free the resonators; the structures were rinsed in methanol, and dried in air. Structures fabricated in this way did not in general collapse, obviating the need for CO_2 critical point drying. An electron micrograph of a set of completed beams in shown in Fig. 1. Note that the narrow part of the beams is completely undercut, while the wider steps are undercut to a depth of approximately 0.3 μm. We take the nominal length L of the beam to be the length measured from the edge of the undercut at either end; the lengths for the beams we describe here ranged from 3.9 to 5.6 μm.

Electrical contacts to the completed resonators were made with Au wire bonds, and the structures were placed in a vacuum can, which was evacuated and then submerged in liquid helium, in the bore of an 8 T magnet. A semirigid 50 Ω coaxial cable connected room-temperature electronics to each resonator. The center pin of the cable was connected to one end of each resonator, with the other end of the resonator grounded. The resonators were oriented with the plane of the sample parallel to the magnetic field, with the beam length perpendicular to the field B, allowing magnetomotive measurement of the beam resonance frequency Ω and quality factor Q.[5] A typical measurement is shown in Fig. 2 for a 3.3 μm long beam, displaying clear resonance at $\Omega/2\pi$

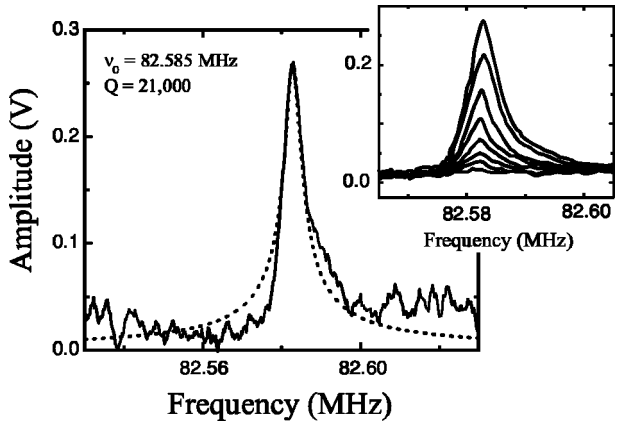

FIG. 2. Measured resonance of a 3.9 μm long beam, measured at 4.2 K in a transverse magnetic field of 8 T. The applied rf power was -85 dBm. Inset: Measured resonance for a constant rf power of -75 dBm, while varying the magnetic field through integer values from 1 T (smallest peak) to 8 T (largest peak).

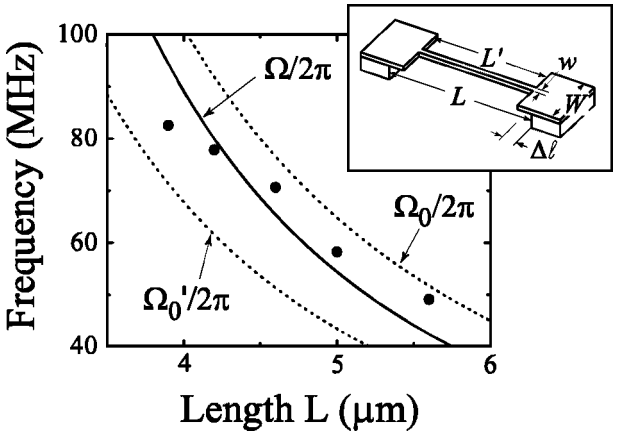

FIG. 3. Measured resonance frequencies for five beam lengths (closed points), with calculated resonance frequencies $\Omega_0(L)/2\pi$ using the nominal beam length L (dotted line), $\Omega_0'(L)/2\pi$ adjusted for Au mass loading (dashed line), and $\Omega/2\pi$ using the numerically calculated frequency accounting for the stepped beam width (solid line). Inset: Geometry defining the beam width $w=0.12$ μm, step width $W=2.4$ μm, nominal length L and effective length $L'=L-2\Delta\ell$.

$=82$ MHz with a quality factor $Q=2.1\times10^4$. Varying the magnetic field for a fixed rf drive power shows the expected quadratic dependence on magnetic field, shown in the inset in Fig. 2.

We measured a number of resonators with different beam lengths but fixed widths; the measured dependence of resonance frequency on nominal beam length L is shown in Fig. 3, along with three theoretical curves.

The resonance frequency Ω for a flexural beam of thickness t, width w and length L is given by solving the Euler–Bernoulli beam equation,

$$-\rho A\Omega^2 Y=\frac{\partial^2}{\partial x^2}EI\frac{\partial^2 Y}{\partial x^2}, \tag{1}$$

where $Y(x)$ is the displacement along the thickness axis, x is measured along the beam length, ρ and E are the density and elastic modulus, $A=wt$ the cross-sectional area, and $I=wt^3/12$ the bending moment of inertia; these parameters can be position dependent.

For a doubly clamped beam with uniform material and geometric parameters, Eq. (1) yields solutions with the natural resonance frequency $\Omega_0(L)$ given by

$$\frac{\Omega_0(L)}{2\pi}=1.027\sqrt{\frac{E}{\rho}}\frac{t}{L^2}. \tag{2}$$

The elastic modulus for an AlN beam with length along the $\langle1000\rangle$ crystal direction and flexure in the $\langle0001\rangle$ direction is given by $E=(c_{11}-c_{12})(c_{11}+2c_{12})/(c_{11}+c_{12})=280$ GPa.[1,10,14] This predicted curve is shown as a dotted line in Fig. 3.

The resonators include a thin Au film, with $\rho=19320$ kg/m^3 and $E=78$ GPa (the Ti wetting layer has a negligible effect). The main effect of the metal is to mass load the resonator, reducing its frequency from that given by Eq. (2). For the large ratio of AlN thickness t_1 to the metal thickness t_2, the resonance frequency for the composite structure is approximately[10]

$$\frac{\Omega_0'(L)}{2\pi} \approx 1.027 \frac{E_1}{\rho_1} \frac{1}{\sqrt{1+\rho_2 t_2/\rho_1 t_1}} \frac{t_1}{L^2}. \quad (3)$$

By evaluating Eq. (3) for our structures, we find a mass-loaded frequency $\Omega_0'(L) \approx 0.67\,\Omega_0(L)$, in terms of the bare resonance frequency $\Omega_0(L)$. This curve is plotted as a dashed line in Fig. 3.

A second correction involves the fact that the beams are not uniform in width along the suspended length, but comprise a 0.2 μm wide section of length L', followed by a short section with width 2.4 μm and undercut length $\Delta\ell = 0.3\,\mu$m at either end. The nominal length L is given by $L = L' + 2\Delta\ell$. One way to approximate the effect of the width increase is to take the effective length L' in Eqs. (2) and (3), assuming that the wider section of the beam is rigidly clamped. However, the increase in beam stiffness provided by the width increase is not equivalent to clamping the beam, so this does not yield an accurate result.

We therefore used a version of Stodola's iterative method,[15] in which the flexure equation, Eq. (1), is solved numerically for the actual beam geometry, yielding an excellent approximation to the actual mode shape $Y(x)$. The resonance frequency may then be evaluated using Rayleigh's method.[16] We have applied this technique to the beam geometry shown in the inset in Fig. 3. The resulting corrections are $\Omega(L)/\Omega_0'(L) = 1.26-1.41$; the correction varies with the proportion $\Delta\ell/L$. In Fig. 3 we show this calculated frequency as a solid line, showing a fairly good correspondence to the measured dependence, with no adjustable parameters.

In conclusion, we have described the fabrication and measurement of high frequency nanomechanical beams, fabricated from single-crystal AlN and measured using a magnetomotive technique. In addition, we find that we can fairly accurately account for the beam frequencies when adjusting for mass loading and for the specific beam geometry. Applications of these types of structures to piezoelectrically driven and detected beam resonances are presently underway.

The authors gratefully acknowledge the support provided by National Science Foundation XYZ-on-a-Chip award, Award No. ECS-9980734, the Army Research Office under Contract No. DAAD-19-99-1-0226, and by a Research Corporation Research Innovation Award.

[1] O. Ambacher, J. Phys. D **31**, 2653 (1998).
[2] J. R. Mileham, S. J. Pearton, C. R. Abernathy, J. D. Mackenzie, R. J. Shul, and S. P. Kilcoyne, J. Vac. Sci. Technol. A **14**, 836 (1995).
[3] Z. Zhang and N. MacDonald, J. Microelectromech. Syst. **2**, 66 (1993).
[4] N. MacDonald, Microelectron. Eng. **32**, 49 (1996).
[5] A. Cleland and M. Roukes, Appl. Phys. Lett. **69**, 2653 (1996).
[6] A. Cleland and M. Roukes, Nature (London) **320**, 160 (1998).
[7] C. Nguyen and R. Howe, Proc. IEEE **48**, 127 (1994).
[8] K. Wang, A. Wong, and C. Nguyen, J. Microelectromech. Syst. **9**, 347 (2000).
[9] R. Beck, M. A. Eriksson, M. A. Topinka, R. M. Westervelt, K. D. Maranowski, and A. C. Gossard, Appl. Phys. Lett. **73**, 1149 (1998).
[10] Y. T. Yang, K. L. Ekinci, X. M. H. Huang, L. M. Schiavone, M. L. Roukes, C. A. Zorman, and M. Mehregany, Appl. Phys. Lett. **78**, 162 (2001).
[11] C. Tran, R. Karlicek, Jr., M. Schurman, T. Salagaj, R. Cassidy, I. Ferguson, A. G. Thompson, R. A. Stall, and C.-Y. Hwang, J. Cryst. Growth **174**, 647 (1997).
[12] T. C. Inc.
[13] E. Williams and R. Muller, J. Microelectromech. Syst. **5**, 256 (1996).
[14] B. Auld, *Acoustic Fields and Waves in Solids* (Wiley, New York, 1973), Vol. I.
[15] J. D. Hartog, *Mechanical Vibrations* (Dover, New York, 1985).
[16] S. Timoshenko, D. Young, and J. W. Weaver, *Vibration Problems in Engineering* (Wiley, New York, 1974).